PHYSICAL REVIEW E, VOLUME 65, 015601(R)

Transverse instability of incoherent solitons in Kerr media

Juan P. Torres,[1,2] Charalambos Anastassiou,[2,3] Mordechai Segev,[2,3] Marin Soljačic,[4] and Demetrios N. Christodoulides[5]
[1]*Department of Signal Theory and Communications, Polytechnic University of Catalonia, 08034 Barcelona, Spain*
[2]*Physics Department and the Solid State Institute, Technion, Haifa 32000, Israel*
[3]*Electrical Engineering Department, Princeton University, Princeton, New Jersey 08544*
[4]*Physics Department, Massachusetts Institute of Technology, Cambridge, Massachusetts 02139*
[5]*Department of Electrical Engineering and Computer Science, Lehigh University, Bethlehem, Pennsylvania 18015*
(Received 29 December 2000; published 7 December 2001)

We calculate the growth rate of the small-amplitude perturbations superimposed on a one-dimensional soliton that is fully coherent in the self-trapping dimension, yet uniform and partially incoherent in the other transverse dimension. Such solitons become transversely stable only if the correlation distance is below a specific threshold value. We show that this threshold for transverse instability fully coincides with the threshold value for modulational instability.

DOI: 10.1103/PhysRevE.65.015601 PACS number(s): 42.65.Tg, 05.45.Yv

Localized light beams broaden during propagation in linear media due to the effect of diffraction. In nonlinear media, this broadening may be counterbalanced, resulting in self-trapped optical beams, i.e., spatial solitons, beams that do not change their shape during propagation. Coherent spatial solitons have been demonstrated experimentally for many nonlinearities, such as Kerr, photorefractive and quadratic [1,2]. Generally speaking, the formation of coherent solitons is closely related to modulational instability (MI), the process in which a plane wave launched in a nonlinear medium breaks up into a train of filaments. MI is also related to another phenomenon that characterizes solitons, transverse instability (TI). For example, coherent $(1+1)$-dimensional $[(1+1)\mathrm{D}]$ solitons, where $(m+1)\mathrm{D}$ means the beam may diffract in m dimensions as it propagates in one dimension, suffer from TI [3,4]. This means that a $(1+1)\mathrm{D}$ soliton that is self trapped in the x dimension and is uniform in the y dimension, breaks up along the y dimension into an array of 2D filaments. Thus, the observation of $(1+1)\mathrm{D}$ spatial solitons requires limiting the diffraction to one transverse dimension. This may be achieved by launching the soliton in planar wave-guide geometries so that diffraction is avoided in the y dimension [5–7]. Saturation of the nonlinear response has been shown to arrest TI [8,9], which enables the observation of $(1+1)\mathrm{D}$ solitons in bulk media for several diffraction lengths [10], although saturation cannot eliminate TI.

For a long time, optical spatial solitons were thought of only as coherent entities. Recently, the existence of incoherent solitons was demonstrated [11]. These are localized incoherent light beams that can exist when the nonlinear time response of the medium is slower than the random fluctuations of the optical field. Modulational instability can also occur with incoherent plane waves [12], but for such incoherent MI to exist, the nonlinearity should be above a well-defined threshold determined by the degree of coherence of the plane wave. This elimination of incoherent MI and the existence of incoherent elliptical solitons with different coherence properties in the x and y dimensions [13], were the clue that drove us to show that it is possible to produce $(1+1)\mathrm{D}$ solitons that do not suffer from TI [14]. The idea was to create a soliton that is fully coherent and self-trapped in x and partially incoherent in y. Since the nonlinearity required for trapping is determined by the properties of the beam along x, the incoherence along y may be increased until the nonlinearity is below threshold and TI is eliminated. In this Rapid Communication, we calculate the growth rate of the transverse perturbations of $(1+1)\mathrm{D}$ incoherent solitons and the threshold of the degree of coherence for the elimination of incoherent TI. In particular, we prove, numerically, that for Kerr media, the threshold value for TI coincides with the threshold for incoherent MI, irrespective of the shape of the coherence function.

In [14], the analysis of the TI of the one-dimensional soliton solution was made with the help of the mutual coherence function. In the onset of elimination of the TI, i.e., at the TI threshold, this function takes a simpler form that allows the calculation of the degree of coherence for the elimination of TI. But the analytic calculation that was presented in [14] could predict only the TI threshold, and nothing else, especially not the full gain curve, that is, the growth rate as a function of spatial frequency and as a function of the correlation function. Furthermore, one could naively think that perhaps it is possible to carry out a numerical calculation following the 1D equations presented in [14]. But even that is not trivial: the full analysis of TI of the one-dimensional soliton solution is cumbersome and expensive computationally within the framework presented there.

Here, we use a different approach, and work out the TI calculation within the coherence density approach, which is much more convenient numerically and is completely equivalent to the mutual coherence density approach [15]. This approach allows us to calculate the entire growth rate curve for the unstable modes. Moreover, we can check the assumptions made in [14] to calculate the degree of coherence for the elimination of TI.

We consider the transverse instability of incoherent one-dimensional Kerr solitons in the framework of the coherent density method [16]. The linearly polarized beam propagating in the z direction is assumed to be incoherent in the y dimension and coherent in the x dimension. The coherent

density function f evolves according to the following normalized nonlinear integro-differential equation:

$$i\frac{\partial f}{\partial \zeta}+i\,\delta\theta\frac{\partial f}{\partial \eta}+\frac{1}{2}\left[\frac{\partial^2 f}{\partial \eta^2}+\frac{\partial^2 f}{\partial s^2}\right]+If=0, \tag{1}$$

where the time-averaged normalized beam intensity I is given by $I(s,\eta,\zeta)=\int_{-\infty}^{\infty}d\theta|f(s,\eta,\theta,\zeta)|^2$ and at $\zeta=0$, the coherent density f is given by $f(s,\eta,\zeta=0)=G^{1/2}(\theta)\Psi_0(s,\eta)$ where $G(\theta)$ is the normalized angular power spectrum of the beam, which is incoherent in η, yet fully coherent in s, and $\Psi_0(s,\eta)$ is the input spatial modulation function. In the above equations, we have used the following normalizations: $s=x/x_0$, $\eta=y/x_0$, where x_0 is an arbitrary beam width, $\zeta=z/(k_0n_0x_0^2)$ and $\delta=k_0n_0x_0$. k_0 is the wave number in vacuum and n_0 is the linear refractive index. The beam intensity is normalized to $I_0=(k_0^2x_0^2n_0\alpha)^{-1}$, where α is the nonlinear Kerr coefficient. Equation (1) has a one-dimensional soliton solution $f_0(s,\theta)=u_0(s)G^{1/2}(\theta)\exp(iA^2\zeta/2)$ where $u_0(s)=A\,\mathrm{sech}(As)$, which coincides with the well-known coherent Kerr soliton, multiplied by $G^{1/2}(\theta)$.

In order to analyze the transverse stability of the one-dimensional soliton solution, we seek solutions of Eq. (1) of the form

$$f=[u_0(s)G^{1/2}(\theta)+\Phi(s,\theta,\zeta)\cos(q\eta)]\exp\left(i\frac{A^2}{2}\zeta\right), \tag{2}$$

where q is the normalized spatial frequency of the perturbation. Inserting Eq. (2) into Eq. (1) and linearizing around the soliton solution, we obtain a linear differential equation for Φ,

$$\frac{\partial\Phi}{\partial\zeta}-\frac{i}{2}\frac{\partial^2\Phi}{\partial s^2}+i\left[q\theta+\frac{q^2}{2}+\frac{A^2}{2}\right]\Phi-iu_0^2(s)\Phi$$
$$-iu_0^2(s)G^{1/2}(\theta)\int_{-\infty}^{\infty}d\theta\,G^{1/2}(\theta)[\Phi+\Phi^*]=0. \tag{3}$$

We are only interested in the solutions of Eq. (3) that display exponential growth, i.e., modes with $\Phi(s,\theta,\zeta)=\Phi(s,\theta)\exp(g\zeta)$, where g is the normalized growth rate of the perturbation. If there would be several modes with different values of g, we would be interested in the mode with the largest growth rate, since we expect this mode to dominate the initial evolution of the perturbed soliton solution according to Eq. (1). For $q=0$, solutions of Eq. (3) can be easily obtained. The soliton solution $f_0(s,\theta)$ still remains a soliton under a change of the position of the peak of the soliton (s_0), and under the addition of a global initial phase (ϕ). Thus, perturbations that correspond to a change of position or a global phase change should correspond to perturbations modes with $g=0$. The most general form of $f_0(s,\theta)$ at $\zeta=0$ (the input to the medium) is given by $f_0(s,\theta)=A\,\mathrm{sech}(As+s_0)\exp(i\phi)G^{1/2}(\theta)$. The solution of Eq. (3) for $q=0$ corresponding to a shift of the position of the soliton is $\Phi(s,\theta)\equiv(\partial f_0/\partial s_0)_{s_0=0,\phi=0}=-A\,\mathrm{sech}(As)\tanh(As)G^{1/2}(\theta)$. The solution corresponding to a global phase change is $\Phi(s,\theta)\equiv(\partial f_0/\partial\phi)_{s_0=0,\phi=0}=iA\,\mathrm{sech}(As)G^{1/2}(\theta)$. For $q\neq0$, Eq. (3) should be solved numerically. For that purpose, we solve Eq. (3) for each value of the spatial frequency q with the method described in [17] and [18]. Namely, for a given soliton solution f_0, we solve Eq. (3) with a general nonzero initial condition $\Phi(s,\theta,\zeta=0)$ using a Crank-Nicholson scheme [19]. In general, the input $\Phi(s,\theta,\zeta=0)$ will be composed of several perturbation modes. For large propagation distances, the perturbation with the largest growth-rate g will dominate since the growth is exponential. We determine numerically the propagation distance beyond which the calculated value of g and the profile of the corresponding mode do not change perceptibly. Equation (3) has a first integral for each angular component given by

$$\frac{\partial}{\partial\zeta}\int_{-\infty}^{\infty}ds|\Phi(s,\theta)|^2$$
$$=2G^{1/2}(\theta)\int_{-\infty}^{\infty}ds\,\mathrm{Im}[\Phi(s,\theta)]u_0^2(s)F(s), \tag{4}$$

where $F(s)=2\int_{-\infty}^{\infty}d\theta\,G^{1/2}(\theta)\mathrm{Re}[\Phi(s,\theta)]$. This first integral is used for checking the numerics of the calculations.

We consider typical experimental values. If we choose a normalization factor $x_0=\omega_0/1.763$, where ω_0 is the full width at half maximum at intensity, the amplitude of the soliton solution of Eq. (1) is $A=1$. The maximum index of refraction change $\Delta n_0=\alpha I_0$, where I_0 is the peak intensity of the soliton solution, is given by $(\Delta n_0/n_0)^{1/2}=1.763\lambda/(2\pi n_0\omega_0)$, where λ is the wavelength of the radiation. For $\lambda=0.5\,\mu$m, $w_0=9\,\mu$m and $n_0=2.3$, we have $\Delta n_0=1.056\times10^{-4}$ and $\delta=147.546$. Figure 1 shows the growth-rate curve for a soliton with $\delta=147.546$. We assume $G(\theta)$ to be Gaussian, i.e., $G(\theta)=(\pi^{1/2}\theta_0)^{-1}\exp(-\theta^2/\theta_0^2)$, where θ_0 is the width of the angular power spectrum. The uppermost curve in Fig. 1, of $\theta_0=0°$, represents a fully coherent beam, and coincides with the result given by Kusnetsov *et al.* [3]. A typical example of the field profile of the calculated perturbations eigenmodes is shown in Fig. 2 for

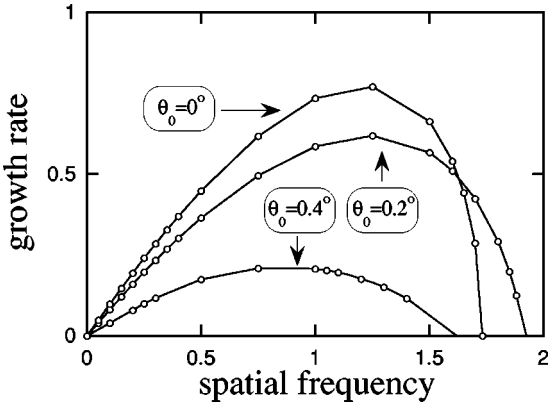

FIG. 1. Growth rate (g) as a function of the spatial frequency (q), both in dimensionless units, for a Gaussian angular power spectrum. Parameters: $A=1$ and $\delta=147.546$. Dots correspond to values calculated numerically by using Eq. (3), while the solid lines are used to help the eye.

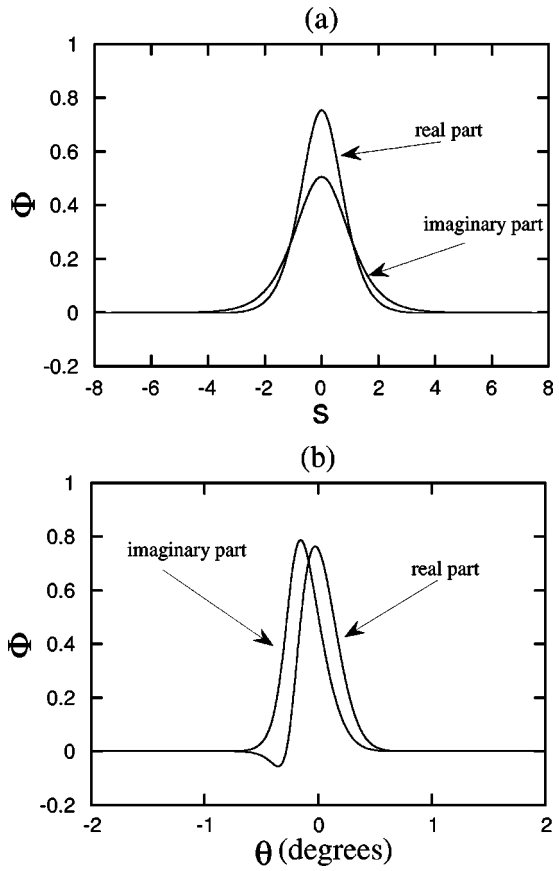

FIG. 2. The profile of the real and imaginary parts of the perturbation Φ with a normalized spatial frequency $q=1.25$, for a Gaussian angular power spectrum with $\theta_0=0.2°$. Parameters: $A=1$ and $\delta=147.546$. (a) Spatial profile and (b) angular profile.

$q=1.25$ and $\theta_0=0.2°$. Notice that the perturbations Φ are symmetric in the s axis, while nonsymmetric in the θ axis. From Fig. 1 we see that the growth-rate curve is diminished as the incoherence θ_0 increases.

It is interesting to observe that, although the maximum gain of the unstable modes diminishes when decreasing the degree of coherence (increasing θ_0), but quite unexpectedly, this does not mean that the region of spatial frequencies for which such instability exists shrinks. In the coherent case, $\theta_0=0°$, the region of instability stops at $q=\sqrt{3}$. When the degree of coherence is decreased, modes with higher spatial frequencies become unstable, as can be readily seen from Fig. 1. But eventually, a further decrease of the degree of coherence reduces the domain of spatial frequencies with gain, arriving to the complete elimination of TI. Once θ_0 reaches a threshold value, the growth rate is no longer real and positive and TI is eliminated. We also observe that to calculate the threshold, all we need to do is to monitor the slope of the growth rate at $q=0$, and see when it goes from positive (θ_0 below threshold) to zero (θ_0 at threshold). The calculation of the threshold value of θ_0 for the elimination of TI following the previous numerical procedure is cumbersome and we seek an alternative way. We will next show numerically that the growth-rate curve for TI and MI for small q coincide and therefore they have the same threshold.

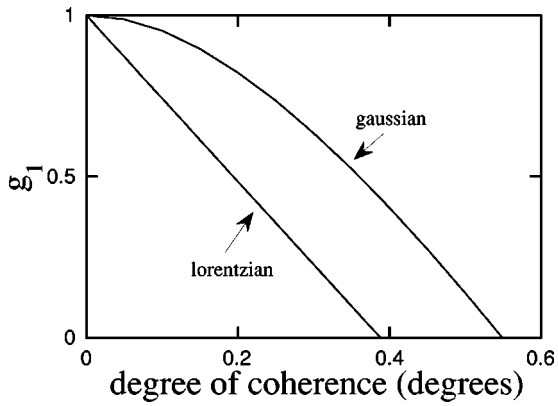

FIG. 3. Slope of the normalized growth-rate curve for MI in the long-wave limit ($q=0$), as a function of the degree of coherence (θ_0). Both a Gaussian and a Lorentzian angular power spectrum are considered. Parameters: $A=1$ and $\delta=147.546$.

This will enable us to obtain the threshold for TI by solving the much simpler analytically solvable problem of MI.

Modulational instability of partially coherent beams has been recently addressed, and the threshold condition for a Lorentzian angular power spectrum was calculated [12]. The MI calculations are addressed through the evolution of the mutual coherence function [20]. Following the method of [12] and using the normalizations of this paper, we arrive at

$$\int_{-\infty}^{\infty} d\theta \frac{A^2}{ig+\delta q\theta}\{G(\theta-q/2\delta)-G(\theta+q/2\delta)\}=1, \quad (5)$$

which allows us to calculate the growth-rate curve $g(q)$. Since the threshold for elimination of MI is related to the slope of the growth-rate curve at $q=0$, we expand Eq. (5) in terms of q by using $g=g_1q+g_2q^2\cdots$ In the limit $q\to 0$, we obtain

$$\frac{2A^2}{\sqrt{\pi}\theta_0^3\delta^2}\int_{-\infty}^{\infty} d\theta \frac{\theta^2}{\theta^2+(g_1/\delta)^2}\exp\left(-\frac{\theta^2}{\theta_0^2}\right)=1, \quad (6)$$

for a Gaussian angular power spectrum, and

$$\frac{2A^2\theta_0}{\pi\delta^2}\int_{-\infty}^{\infty} d\theta \frac{\theta^2}{\theta^2+(g_1/\delta)^2}\frac{1}{(\theta^2+\theta_0^2)^2}=1, \quad (7)$$

for a Lorentzian angular power spectrum, i.e., $G(\theta)=(\theta_0/\pi)(\theta^2+\theta_0^2)^{-1}$. Figure 3 shows the value of g_1 as a function of the degree of coherence θ_0 for both the Gaussian and Lorentzian angular power spectrum. For $\theta_0=0°$, we recover the coherent limit i.e., $g_1=A$. The curve for the Lorentzian case coincides with the appropriate limit of the corresponding expression given in [12], which was calculated with an alternative method.

As can be readily observed in Fig. 3, the slope of the growth-rate curve near $q=0$ (g_1), depends on the specific form of the profile of the angular power spectrum, so it does depend on the degree of coherence for the elimination of TI. At threshold, $g_1=0$ and the evaluation of the integrals in Eqs. (6) and (7) give the threshold condition $\theta_0=\sqrt{2}A/\delta$ for

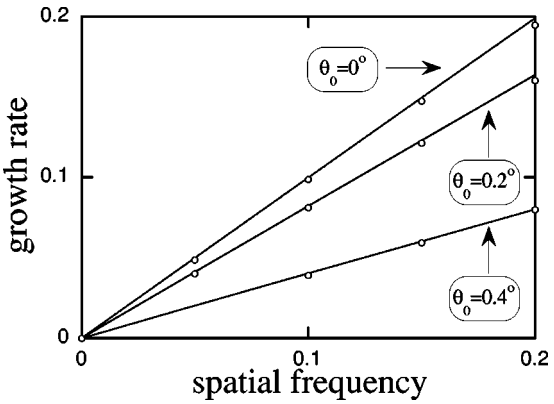

FIG. 4. Comparison of the growth rate for TI (dots) and for MI (solid lines) for small values of q, for several values of the degree of coherence θ_0. The growth rate and the spatial frequency are in dimensionless units. The angular power spectrum is Gaussian. Parameters: $A=1$ and $\delta=147.546$.

the Gaussian angular power spectrum and $\theta_0=A/\delta$ for the Lorentzian one. Figure 4 shows the comparison between the growth-rate curve for TI near $q=0$ calculated using Eq. (3) and the growth-rate curve for MI calculated using Eq. (6), for a Gaussian angular power spectrum. Only small values of the spatial frequency, where this comparison is meaningful, are considered. The curves drawn in Fig. 4 show us that the slope of the growth-rate curve at the long-wavelength limit for both the MI and TI cases is the same, so the threshold value obtained for MI applies as well to TI.

We should note that coherent TI and MI in the long-wavelength limit also coincide. In the case of coherent MI the growth-rate g is given [21] by $g(q)=(A^2q^2-q^4/2)^{1/2}$. By expanding this expression for small values of q, we obtain $g\simeq Aq$. In the case of coherent TI, the growth-rate curve should be calculated numerically, although in the long-wavelength limit, the growth rate may be shown to go as $g(q)\simeq Aq$ [3]. Notice that both MI and TI should coincide at $q=0$, since in both cases, a small uniform change of amplitude or phase correspond to the modes with $q=0$ and zero growth rate [22].

To conclude, we have calculated the growth-rate curve for the transverse perturbations upon a one-dimensional Kerr soliton that is fully coherent in the self-trapping direction, yet uniform and partially coherent in the other transverse dimension. We have shown that the threshold for transverse instability, above which the beam breaks up into 2D filaments, fully coincides with the threshold value for modulational instability of uniform-intensity plane waves of the same coherence function. We have proven that, for Kerr media, the threshold value of TI and MI coincide for Kerr solitons, irrespective of the shape of the transverse coherence function. Furthermore, we conjecture that the coincidence of the TI and MI threshold values holds for any form of nonlinearity. This carries much importance, because the MI threshold value can always be readily calculated analytically [12,14], whereas the TI growth-rate curve requires extensive numerical simulations.

[1] G. I. Stegeman and M. Segev, Science **286**, 1518 (1999).
[2] N. N. Akhmediev and A. Ankiewicz, *Solitons: Nonlinear Pulses and Beams* (Chapman and Hall, London, 1997).
[3] E. A. Kuznetsov, A. M. Rubenchik, and V. E. Zakharov, Phys. Rep. **142**, 105 (1986).
[4] Y. S. Kivshar and D. E. Pelinovsky, Phys. Rep. **331**, 117 (2000).
[5] A. Barthelemy, S. Maneuf, and C. Frohly, Opt. Commun. **55**, 201 (1985).
[6] J. S. Aitchinson, A. M. Weiner, Y. Silberberg, M. K. Oliver, J. L. Jackel, C. E. Leaird, E. M. Vogel, and P. W. E. Smith, Opt. Lett. **15**, 471 (1990).
[7] R. Schiek, Y. Baek, and G. I. Stegeman, Phys. Rev. E **53**, 1138 (1996).
[8] N. Akhmediev, V. Korneev, and R. Nabiev, Opt. Lett. **17**, 393 (1992).
[9] Z. Musslimani, M. Segev, A. Nepomnyashchy, and Y. Kivshar, Phys. Rev. E **60**, R1170 (1999).
[10] K. Kos, H. Meng, G. Salamo, M. Shih, M. Segev, and G. Valley, Phys. Rev. E **53**, R4330 (1996).
[11] M. Mitchell, Z. Chen, M. Shih, and M. Segev, Phys. Rev. Lett. **77**, 490 (1996).
[12] M. Soljacic, M. Segev, T. Coskun, D. N. Christodoulides, and A. Vishwanath, Phys. Rev. Lett. **84**, 467 (2000).
[13] E. Eugenieva, D. N. Christodoulides, and M. Segev, Phys. Rev. Lett. **25**, 972 (2000).
[14] C. Anastassiou, M. Soljacic, M. Segev, E. D. Eugenieva, D. N. Christodoulides, D. Kip, Z. Musslimani, and J. P. Torres, Phys. Rev. Lett. **85**, 4888 (2000).
[15] D. M. Christodoulides, E. D. Eugenieva, T. H. Coskun, M. Segev, and M. Mitchell, Phys. Rev. E **63**, 035601(R) (2001).
[16] D. M. Christodoulides, T. H. Coskun, M. Mitchell, and M. Segev, Phys. Rev. Lett. **78**, 646 (1997).
[17] N. N. Akhmediev, V. I. Korneev, and Y. V. Kuzmenko, Sov. Phys. JETP **61**, 62 (1985).
[18] J. M. Soto-Crespo, D. R. Heatley, E. M. Wright, and N. N. Akhmediev, Phys. Rev. A **44**, 636 (1991).
[19] W. H. Press, B. P. Flannery, S. A. Teukolsky, and W. T. Vetterling, *Numerical Recipes* (Cambridge University Press, Cambridge, 1992).
[20] V. V. Shkunov and D. Z. Anderson, Phys. Rev. Lett. **81**, 2683 (1998).
[21] G. P. Agrawal, *Nonlinear Fiber Optics* (Academic, San Diego, 1989).
[22] Y. Lai, J. Opt. Soc. Am. B **10**, 475 (1993).